Acta Biochim Biophys Sin 2011, 43: 977–988 | © The Author 2011. Published by ABBS Editorial Office in association with Oxford University Press on behalf of the Institute of Biochemistry and Cell Biology, Shanghai Institutes for Biological Sciences, Chinese Academy of Sciences. DOI: 10.1093/abbs/gmr095.
Advance Access Publication 25 October 2011

Original Article

Structural insights into the homology and differences between mouse protein tyrosine phosphatase-sigma and human protein tyrosine phosphatase-sigma

Li Hou[1†], Jianchuan Wang[2†], Yueyang Zhou[3], Jingya Li[3], Yi Zang[3*], and Jia Li[1,3*]

[1]School of Life Science, East China Normal University, Shanghai 200062, China
[2]State Key Laboratory of Molecular Biology and Research Center for Structural Biology, Institute of Biochemistry and Cell Biology, Shanghai Institutes for Biological Sciences, Chinese Academy of Sciences, Shanghai, China
[3]National Center for Drug Screening, Shanghai Institute of Materia Medica, Chinese Academy of Sciences, Shanghai 201203, China
[†]These authors contributed equally to this work.
*Correspondence address. Tel: +86-21-50801313-208; Fax: +86-21-50800721; E-mail: yzang@mail.shcnc.ac.cn (Y.Z.)/Tel: +86-21-50801313-341; Fax: +86-21-50800721; E-mail: jli@mail.shcnc.ac.cn (J.L.)

Protein tyrosine phosphatases PTP-sigma (PTPσ) plays an important role in the development of the nervous system and nerve regeneration. Although cumulative studies about the function of PTPσ have been reported, yet limited data have been reported about the crystal structure and *in vitro* activity of mouse PTPσ. Here we report the crystal structure of mouse PTPσ tandem phosphatase domains at 2.4 Å resolution. Then we compared the crystal structure of mouse PTPσ with human PTPσ and found that they are very similar, superimposing with a root mean square deviation of 0.45 Å for 517 equivalent Cα atoms. But some residues in mouse PTPσ form loops while corresponding residues in human PTPσ form β-sheets or α-helices. Furthermore, we also compared *in vitro* activities of mouse PTPσ with human PTPσ and found that mouse PTPσ has 25-fold higher specific activity than human PTPσ does toward O-methyl fluorescein phosphate (OMFP) as the substrate. However, there is no significant activity difference between the mouse and the human enzyme detected with *p*-nitrophenylphosphate (pNPP) as the substrate. Mouse PTPσ and human PTPσ have different substrate specificities toward OMFP and pNPP as substrates. This work gives clues for further study of PTPσ.

Keywords mouse PTP-sigma; crystallization; homology; difference

Received: July 13, 2011 Accepted: September 2, 2011

Introduction

Protein tyrosine phosphatases (PTPs), in coordination with protein tyrosine kinases, play essential regulatory roles in diverse cellular activities by modulating the phosphorylation state of target proteins [1]. Dysregulation of PTPs is associated with a multitude of diseases, such as cancers, diabetes, allergic inflammation, and nervous system diseases [2–7]. Many members of the PTP family have been identified as potential therapeutic targets [8]. The human genome contains 107 PTP genes, with the Class I cysteine-based PTP genes constituting the largest group. This group can be further subdivided into 61 dual-specificity phosphatases and 38 tyrosine-specific PTP genes, the 'classical PTPome'. Classical PTPs have been further subdivided into receptor (R1–R8) and non-transmembrane (NT1–NT9) subgroups [9,10]. Twelve receptor PTPs contain two catalytic domains (tandem domains), while the remaining PTPs only have a single catalytic phosphatase domain. In tandem-domain receptor protein tyrosine phosphatases (RPTPs), it is the PTP (D1) domain adjacent to the plasma membrane that displays catalytic activity while the PTP (D2) domain is either inactive or has negligible catalytic activity [10].

PTP-sigma (PTPσ) belongs to the Type R2A sub-family of receptor PTPs. Other members of this sub-family include the human leukocyte common antigen-related PTP (LAR), PTPdelta (PTPδ), the invertebrate ortholog Dlar, DPTP69D in *Drosophila*, PTP-3 in *Caenorhabditis elegans*, and HmLAR1/2 in *Hirudo medicinalis* [11]. PTPσ and other members of the Type R2A sub-family play vital roles in the central and peripheral nervous systems by providing and responding to axon guidance, synaptic function, and nerve repair [7,12–15]. By using brain lysate from PTPσ-deficient mice, in combination with substrate trapping experiments, N-cadherin and β-catenin were identified as substrates of PTPσ, which led to a model of PTPσ-regulated axon growth involving a cadherin/catenin-dependent pathway [16]. In addition, PTPσ inhibits axonal regeneration and the rate of axon extension [17]. The rate of nerve regeneration is enhanced after trauma (e.g., crush or transection) in PTPσ-deficient mice [18]. In addition,

PTPσ acts as a receptor for chondroitin sulfate proteoglycan, an inhibitor of neural regeneration, which clarifies the nerve regeneration inhibitory mechanism of chondroitin sulfate proteoglycan [19]. The contributions to axon growth and regeneration make PTPσ become an interesting and important phosphatase.

Therefore, investigation of the activity and structure of PTPσ may provide clues for further understanding this protein. Although the three-dimensional structure of human PTPσ tandem phosphatase domains has been determined at 2.0 Å [11], limited studies about mouse PTPσ structure and *in vitro* activity have been done. Here, we report the crystal structure of mouse PTPσ tandem phosphatase domains at 2.4 Å resolution and present a straightforward structural insight as well as *in vitro* activity basis for homology and difference between mouse PTPσ and human PTPσ. It was found that mouse PTPσ and human PTPσ have different substrate specificities targeting O-methyl fluorescein phosphate (OMFP) and *p*-nitrophenylphosphate (pNPP).

Materials and Methods

Expression and purification of recombinant proteins

The tandem phosphatase domains of mouse PTPσ (abbreviated as mPTPσ-D1D2, residues 1326–1907, ref NP_035348.2) were amplified by PCR with pGEX-KG/mPTPσ (kindly donated by Prof. Michel Tremblay, McGill Cancer Centre and Department of Biochemistry, McGill University, Montréal, Canada) as the template. The amplified cDNA was cloned into *Nde*I and *Bam*HI sites of the pET21b vector. The equivalent construction of human PTPσ (abbreviated as hPTPσ-D1D2, residues 1329–1910, ref NP_570924.2) was operated using the same method as above but the PCR template was cDNA encoding human PTPσ, which was purchased from Open Biosystem (Thermo Fisher Scientific, Rockford, USA). Then membrane proximal domains of mouse PTPσ (abbreviated as mPTPσ-D1, residues 1326–1637, ref NP_035348.2) and human PTPσ (abbreviated as hPTPσ-D1, residues 1329–1640, ref NP_570924.2) were cloned with the pET21b-mPTPσ-D1D2 and the pET21b-hPTPσ-D1D2 as templates respectively, using the same clone sites with mPTPσ-D1D2 plasmid. The mutants of mPTPσ-D1 were constructed using the Quik-Change Site-directed Mutagenesis Kit (Stratagene, La Jolla, USA) as directed by the manufacturer with the pET21b-mPTPσ-D1 as the template. All constructs were verified by DNA sequencing.

The recombinant plasmids were transformed into *Escherichia coli* strain BL21(DE3)pLysS cells. The cells containing plasmids were grown at 37°C in Luria-Bertani medium supplemented with 50 μg/ml of ampicillin till OD_{600} value reached 1.0 and then induced with 0.1 mM isopropyl β-*D*-1-thiogalactopyranoside for further 10 h at 30°C. The cells were harvested by centrifugation and resuspended in buffer A (20 mM Tris-HCl, pH 8.0). The suspension was then lysed by sonication on ice. After centrifugation, the resultant supernatant was loaded onto the Ni-NTA agarose (Qiagen, Hilden, Germany), which was pre-equilibrated with buffer A. Then the His6-tagged proteins were eluted with an elution buffer (buffer A supplemented with 50 mM imidazole). The eluted fractions were then loaded onto a HiTrap Q anion exchange column (GE Healthcare, Wisconsin, USA) and the target protein was eluted in fractions containing buffer A with 300–500 mM NaCl. For crystallization, the eluted fractions were pooled together and further purified by gel filtration with a Sephacryl S-200 column (GE Healthcare) pre-equilibrated with buffer B [10 mM Hepes, pH 7.5, 150 mM NaCl, 10 mM methionine, 10% glycerol, and 2 mM DL-dithiothreitol (DTT)]. Fractions containing target proteins were pooled and concentrated. For kinetic assay, target proteins eluted from the HiTrap Q anion exchange column were desalted into buffer C (20 mM Tris-HCl, pH 8.0, 260 mM NaCl, and 2 mM DTT) with a HiPrep 26/10 desalting column (GE Healthcare). Protein concentrations were determined by the Bradford method with bovine serum albumin as the standard. Protein purities and homogeneities were determined by sodium dodecyl sulfate polyacrylamide gel electrophoresis (SDS–PAGE).

Crystallization and diffraction data collection

Crystallization was performed at 4°C using the hanging-drop vapor diffusion method. The protein samples were concentrated to ~8 mg/ml before crystallization. Bean-shaped crystals were grown in drops containing equal volumes (2 μl) of the protein mixture solution and the reservoir solution (0.08 M malic acid or 0.08 M succinic acid, pH 7.0, 15% PEG3350) to the maximum size in 2–3 days. Diffraction data were collected to 2.4 Å resolution from flash-cooled crystals at −176°C at beamline BL-17U in the Shanghai Synchrotron Radiation Facility (Shanghai, China) and processed with the HKL2000 suite [20]. A summary of the diffraction data statistics is shown in **Table 1**.

Structure determination and refinement

The structure was solved with the molecular replacement method implemented in the program suite CCP4 using the structure of the human PTPσ (PDB code 2FH7) as the model. The initial structure refinement was carried out with program CNS [21,22] and REFMAC5 following the standard protocol. Model building was performed manually with the program COOT [23]. Throughout the refinement, 5% of randomly chosen reflection were set aside for free *R* factor

Table 1 Crystallographic data and refinement statistics

Item	Data
Statistics of diffraction data	
Space group	$P6_1$
Cell parameters	a = b = 94.7 Å c = 124.2 Å
Resolution range (Å)	50.0–2.40 / (2.49–2.40)
Observed reflections	139919
Unique reflections	22320
Average redundancy	6.3 (5.5)
Average I/σ (I)	20.8 (3.4)
Completeness (%)	90.3 (92.5)
R merge (%)	7.2 (43.4)
Statistics of refinement model	
Number of reflections	
Working set	21203
Free R set	1117
R factor/free R factor (%)	23.3/27.2
RMS bond lengths (Å)	0.006
RMS bond angles (°)	1.1
Average B factor	66.2
Ramachandran plot (%)	
Most favored regions	87.1
Allowed regions	12.4
Generously allowed regions	0.4
Disallowed regions	0

$R_{\text{factor}} = ||F_o| - |F_c|| / |F_o|$

monitor. The final stereochemical quality of structural model was checked by PROCHECK. A summary of structure refinement is listed in **Table 1**.

Activity assay and kinetic study

The activity assay of PTPσ was carried out in a 50-μl system containing 50 mM CH_3COONa, pH 5.0, 2 mM DTT, 1 mM ethylenediaminetetraacetic acid, 0.1% CHAPS, 10 μM OMFP or 200 mM pNPP, and different PTPσ concentrations (25 nM mPTPσ-D1D2, 100 nM hPTPσ-D1D2, 37.6 nM mPTPσ-D1, 934 nM hPTPσ-D1, and 37.6 nM mPTPσ-D1 mutants). The rate of degradation product, OMF, was shown with the change of emitted light at 535 nm under the exciting light at 485 nm, which was monitored continuously for 5 min, and the initial rate of degradation was determined using the early linear region of the enzymatic reaction curve. Continuous kinetic monitoring was performed in clear 384-well plates (Corning, Lowell, USA) on Envision (Pelkin Elmer Life Sciences, Downers Grove, USA) controlled by Wallac EnVision Manager at room temperature.

The kinetic parameters were analyzed by GraphPad Prism 5.0 (GraphPad Software, La Jolla, USA) and presented as the mean ± SD from at least three independent experiments. The K_m value was calculated in GraphPad Prism using non-linear regression analysis and enzyme kinetics (Michealis–Menten or k_{cat}) equation.

Results

Structure of mPTPσ-D1D2

To crystallize mPTPσ-D1D2, the plasmid carrying *mPTPσ-D1D2* gene was constructed. The recombined protein was purified to crystallization level through the Ni-NTA agarose followed by Q-Sepharose anion exchange and gel filtration S-200 chromatography. Then mPTPσ-D1D2 was crystallized and its structure was solved by molecular replacement at 2.4 Å resolution (PDB code 3SR9). mPTPσ-D1D2 is a monomer in the crystalline state and also behaves as a monomer in solution as judged by analytical gel filtration chromatography (data not shown), which is constant with that of hPTPσ-D1D2 [11]. In the molecule, the fragment contains two well-defined PTP domains, D1 and D2, connected by a 10-residue linker (**Fig. 1**). Both phosphatase domains have the same overall tertiary fold as seen in the previously determined PTP structures [11,24–26]. The main features of each domain include a highly twisted eight-stranded mixed β-sheet flanked by four α-helices on one side and two on the other (**Fig. 1**). The active site topologies within the two mPTPσ domains D1 and D2 are very similar to each other and also similar to the other PTPs, all with a cradle for phosphopeptide binding surrounded by four loop regions (**Fig. 1**). However, Asp-1516 from the WPD loop in D1 changes into Glu-1805 in D2 and Tyr-1381 from the KNRY loop in D1 changes into Leu-1670 in D2, which may account for the altered activity of D2 [24]. As there is no substrate or substrate analogs in the crystal structure, the catalytic (WPD) loop is open, which is consistent with the published crystal structure of hPTPσ-D1D2 [11].

Structural comparison of mPTPσ-D1D2 and other PTPs

After the determination of the crystal structure of mPTPσ-D1D2, structural comparison was made between the two structures of mPTPσ-D1D2 (PDB code 3SR9) and hPTPσ-D1D2 (PDB code 2FH7). The overall structures were proved to be very similar, superimposing with a root mean square deviation (RMSD) of 0.45 Å for 517 equivalent Cα atoms. Moreover, the structure of mPTPσ-D1D2 almost overlaps with hPTPσ-D1D2 (**Fig. 1**). In the overlay shown in **Fig. 1**, the active sites of mPTPσ-D1D2 and hPTPσ-D1D2 are highly structurally conserved. In particular, the residues that form the WPD loop (containing the catalytic acid D), KNRY loop (participating in phosphotyrosine recognition), CX_5R catalytic site motif (capable of

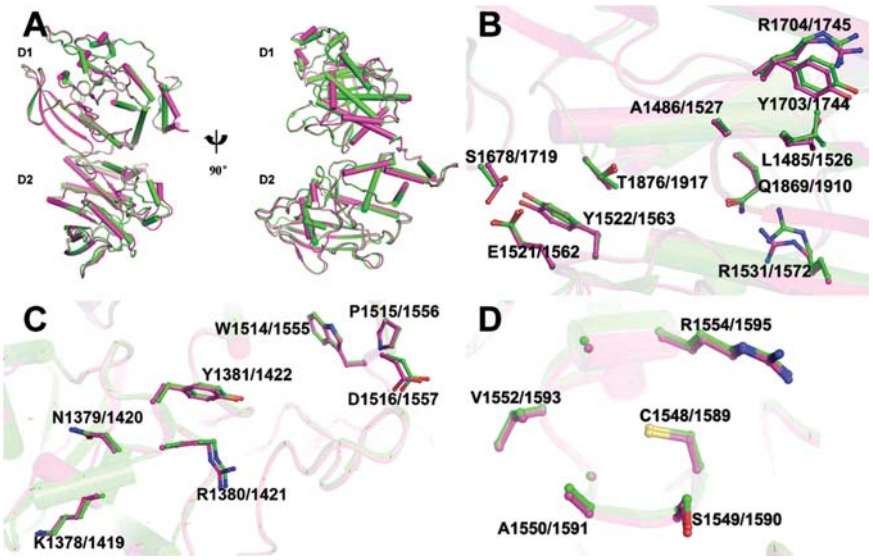

Figure 1 Structural similarities of mPTPσ-D1D2 and hPTPσ-D1D2 mPTPσ-D1D2 and hPTPσ-D1D2 are shown in magenta and green, respectively. (A) Superposition structures of mPTPσ-D1D2 and hPTPσ-D1D2. On the left, the active site of D1 domain is facing the viewer and that of D2 domain is facing rightward. On the right, the same molecule is counterclockwise rotated along the vertical axis ~90°. (B) Amino acids involved in interdomain interactions. (C,D) Active sites comparison of the mPTPσ and hPTPσ D1 domains. Side chains of residues involved in catalysis are shown with sticks and colored by elements. Amino acid residues are shown with oxygen in red, nitrogen in blue, and sulfur in yellow. (C) KNRY loop and WPD loop and (D) CX_5R loop.

binding the phosphate analog tungstate), as well as the interface participating in interaction between D1 and D2 domains are strictly overlapped and the regions around them are nearly invariant. However, there are still some tiny structural differences between mPTPσ-D1D2 and hPTPσ-D1D2. For example, the first β-sheet (residues 1408–1411 aa) of mPTPσ-D1D2 is shorter than the corresponding β-sheet (residues 1446–1454 aa) of hPTPσ-D1D2. Residues 1391–1393 of mPTPσ-D1D2 form a loop but the corresponding residues 1432–1434 in hPTPσ-D1D2 form a β-sheet. Residues 1337–1358 of mPTPσ-D1D2 form two helices but the corresponding residues 1378–1399 in hPTPσ-D1D2 form only one helix. In addition, in D2 domains, residues 1656–1668 of mPTPσ-D1D2 form a loop but the corresponding residues 1697–1709 in hPTPσ-D1D2 form two helices (**Fig. 2**). These structural similarities and differences between the two species PTPσ-D1D2 may bring about corresponding activity similarities or differences.

Besides structural comparison of mPTPσ and hPTPσ, we compared the crystal structure of mPTPσ with other tandem phosphatase domains of LAR, CD45, and PTPγ. As shown in **Fig. 3**, the overall organization of the PTPσ, LAR, CD45, and PTPγ tandem phosphatase domains is very similar. However, it is remarkable that the WPD loop (catalytic loop) of PTPσ is open due to no substrate binding in the crystal structure, which is the same to LAR and PTPγ. But the WPD loop of CD45 is closed because of substrate binding. Detailed comparison of residues participating in catalytic process suggests that the catalytic acid (D) of WPD loop in PTPσ, LAR, and PTPγ is outward of the active center but the catalytic acid (D) of CD45 is inward to the active center, which makes it easier for itself to provide proton for catalytic process. In addition, in PTPσ, LAR, and PTPγ, the position of the basic residue (R) that is important for both substrate binding and transition state stabilization is different from that in CD45. This difference is almost certainly due to substrate binding. It could be speculated from the structural comparison that residues in PTPσ active center, especially the catalytic acid (D) and basic residue (R), are probably to shift in the same way during catalytic process.

Specific activity and kinetic parameters differences between mPTPσ-D1D2 and hPTPσ-D1D2 toward OMFP as the substrate

Structural comparison between mPTPσ-D1D2 and hPTPσ-D1D2 suggests that although the structure of mPTPσ-D1D2 is very similar to that of hPTPσ-D1D2, there are still some tiny structural differences. To investigate whether these differences could bring about activity differences, the recombinant proteins mPTPσ-D1D2 and hPTPσ-D1D2 were purified to high purity and homogeneity through the Ni-NTA agarose followed by Q-Sepharose anion exchange chromatography (**Fig. 4**). Then their activities and kinetic parameters were measured under the same assay conditions (details described in Materials and Methods). Specific activities are relatively high, which are

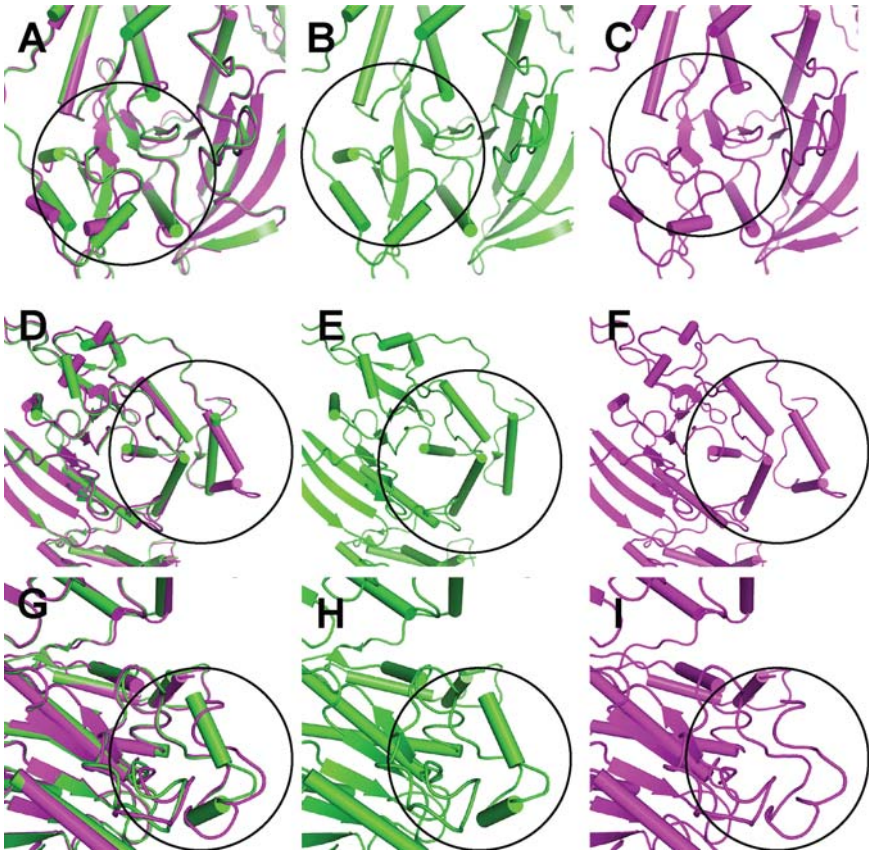

Figure 2 Structural differences between mPTPσ-D1D2 and hPTPσ-D1D2 Crystal structures of mPTPσ-D1D2 and hPTPσ-D1D2 were firstly superimposed and then their secondary structural differences were analyzed. Different enzymes are shown in different colors (mPTPσ-D1D2 in magenta and hPTPσ-D1D2 in green). Black circles are used to highlight regions that are different between mPTPσ-D1D2 and hPTPσ-D1D2. (A–C) Shorter first β-sheet (residues 1408–1411 aa) of mPTPσ-D1D2 compared with the corresponding β-sheet (residues 1446–1454 aa) of hPTPσ-D1D2. (D,E) and (G–I) Helices formation differences between mPTPσ-D1D2 and hPTPσ-D1D2. (D,E) Two helices formed by residues 1337–1358 in mPTPσ-D1D2 but only one helix formed by the corresponding residues 1378–1399 in hPTPσ-D1D2. (G–I) Residues 1656–1668 of mPTPσ-D1D2 form a loop but the corresponding residues 1697–1709 in hPTPσ-D1D2 form two helices in D2 domains.

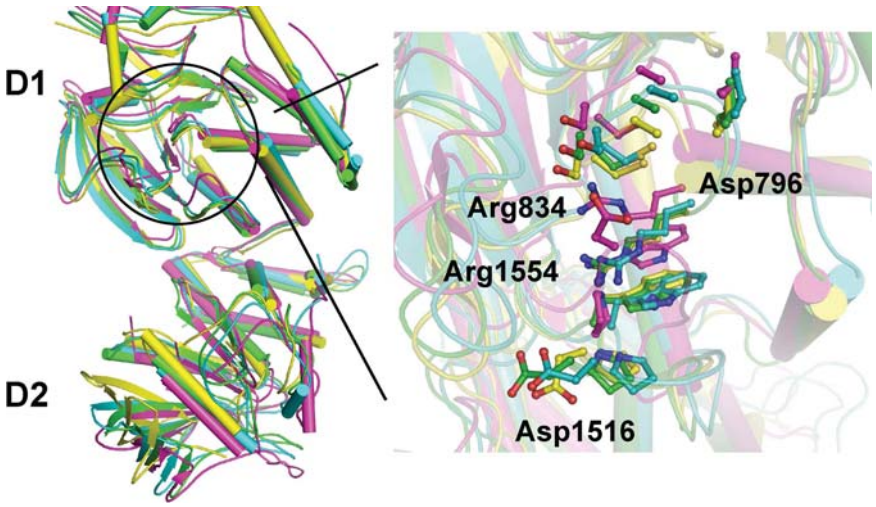

Figure 3 Structural comparison of tandem phosphatase domains of PTPs Superposition of the structures of the tandem phosphatase domains of mouse PTPσ (green), LAR (cyans), CD45 (magenta), and PTPγ (yellow). Key amino acids involved in catalysis are shown with sticks to the right of the D1–D2 structures. Amino acids tagged with names and positions are residues of mouse PTPσ and CD45 (Arg-1554 and Asp-1516 belongs to mouse PTPσ. Arg-834 and Asp-796 belongs to CD45).

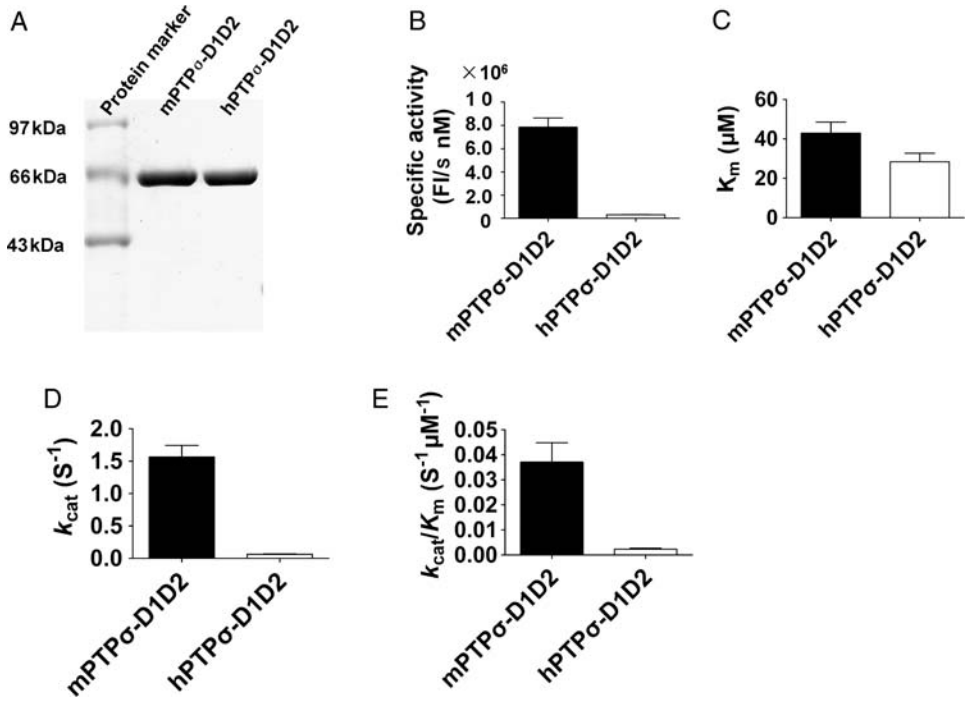

Figure 4 Specific activity and kinetic parameters differences between mPTPσ-D1D2 and hPTPσ-D1D2 toward OMFP as the substrate (A) Purification of mPTPσ-D1D2 and hPTPσ-D1D2. Lane 1 shows low-molecular-weight protein marker; Lanes 2 and 3 are mPTPσ-D1D2 and hPTPσ-D1D2, respectively. Samples were analyzed on a 10% SDS−PAGE and then the gel was stained with Coomassie blue G250. The molecular weight of mPTPσ-D1D2 and hPTPσ-D1D2 is 68 kDa. Purity of them is crystallization level. (B) Specific activity comparison between mPTPσ-D1D2 and hPTPσ-D1D2. The specific activity of mPTPσ-D1D2 is ∼25 folds higher than that of hPTPσ-D1D2. (C) K_m comparison between mPTPσ-D1D2 and hPTPσ-D1D2. K_m of mPTPσ-D1D2 is ∼1.6 folds the amount of hPTPσ-D1D2. (D) k_{cat} comparison between mPTPσ-D1D2 and hPTPσ-D1D2. k_{cat} of mPTPσ-D1D2 is 26 folds as much as that of hPTPσ-D1D2. (E) k_{cat}/K_m comparison between mPTPσ-D1D2 and hPTPσ-D1D2. k_{cat}/K_m of mPTPσ-D1D2 is ∼17 folds higher than that of hPTPσ-D1D2. All data are shown as the mean value ± SD ($n = 3$).

consistent with previous studies [25]. Surprisingly, mPTPσ-D1D2 has 25-fold higher specific activity than hPTPσ-D1D2 does. In addition, kinetic parameters of mPTPσ-D1D2 and hPTPσ-D1D2 were also determined. As shown in **Fig. 4** and **Table 2**, there is almost no difference in K_m between them, which is consistent with the structural similarities in CX_5R catalytic site motifs deep in the active sites. However, k_{cat} of mPTPσ-D1D2 is 25 folds higher than that of hPTPσ-D1D2. The specific activity difference between mPTPσ-D1D2 and hPTPσ-D1D2 might be caused by the difference in catalytic efficiency rather than in the substrate binding ability.

Specific activity and kinetic parameters differences between mPTPσ-D1 and hPTPσ-D1 toward OMFP as the substrate

To clarify the catalytic efficiency difference between mPTPσ-D1D2 and hPTPσ-D1D2, we initially aligned the amino acid sequences of mPTPσ-D1D2 and hPTPσ-D1D2. However, sequences alignment of mPTPσ-D1D2 and hPTPσ-D1D2 showed 96% identity, and residues among active center including WPD loop, KNRY loop, and CX_5R loop are entirely identical. There are only 20 different residues scattered in the sequences (**Fig. 5**). It was reported that it is the PTP (D1) domain adjacent to the plasma membrane that displays catalytic activity while the PTP (D2) domain is either inactive or has negligible catalytic activity in tandem-domain RPTPs [10]. To investigate whether the activity difference in mPTPσ-D1D2 and hPTPσ-D1D2 is induced by mPTPσ-D1 and hPTPσ-D1 activity difference, mPTPσ-D1 and hPTPσ-D1 were purified to have crystallization grade purity (**Fig. 6**) and their specific activities were measured using the same assay as the mPTPσ-D1D2. In agreement with the specific activity difference between mPTPσ-D1D2 and hPTPσ-D1D2, the specific activity of mPTPσ-D1 is ∼19 folds higher than that of hPTPσ-D1. Furthermore, the kinetic parameter differences between mPTPσ-D1 and hPTPσ-D1 are similar to those between mPTPσ-D1D2 and hPTPσ-D1D2. As shown in **Fig. 6** and **Table 3**, K_m of mPTPσ-D1 is ∼1.6 folds as high as that of hPTPσ-D1, but the k_{cat} of mPTPσ-D1 is ∼20 folds as much as that of hPTPσ-D1. Therefore, it could be speculated that the specific activity difference between mPTPσ-D1D2 and hPTPσ-D1D2 toward OMFP as the substrate may be resulted from the difference between mPTPσ-D1 and hPTPσ-D1.

Table 2 Specific activity and kinetic parameters of PTPσ-D1D2 determined with OMFP as the substrate

	Specific activity (FI/s nM)	K_m (μM)	k_{cat} (S^{-1})	k_{cat}/K_m (S^{-1} M^{-1})
mPTPσ-D1D2	$7.8 \times 10^6 \pm 7.9 \times 10^5$	$4.3 \times 10^1 \pm 4.8$	1.6 ± 0.2	$3.7 \times 10^4 \pm 7.7 \times 10^3$
hPTPσ-D1D2	$3.0 \times 10^5 \pm 1.4 \times 10^4$	$2.8 \times 10^1 \pm 3.8$	$6.2 \times 10^{-2} \pm 9.0 \times 10^{-3}$	$2.2 \times 10^3 \pm 5.0 \times 10^2$
mPTPσ-D1D2/ hPTPσ-D1D2	26.0 ± 3.0	1.6 ± 0.5	26.0 ± 7.2	18.1 ± 8.7

Figure 5 Sequences alignment of mPTPσ-D1D2 and hPTPσ-D1D2 mPTPσ and hPTPσ have 96% homology. The numbers indicate the amino acid positions. The standard single-letter code was used. The first box indicates D1 domain and the second represents D2 domain. Sequences between them are linker. Different residues between mPTPσ-D1D2 and hPTPσ-D1D2 are colored in red.

Specific activity comparison among mPTPσ-D1 wild type and mutants

Since the specific activity of mPTPσ-D1 is ~19 folds higher than that of hPTPσ-D1 and sequences alignment suggests that 11 amino acids are different between mPTPσ-D1 and hPTPσ-D1 (**Fig. 5**), we suspected that the different amino acids could induce specific activity or kinetic parameters differences. To solve this problem, the different amino acids in mPTPσ-D1 were mutated to corresponding amino acids in hPTPσ-D1 and recombined proteins were purified to have crystallization grade purity (**Fig. 7**). Then the specific activities were measured using the same assay as in wild-type mPTPσ-D1. As shown in **Fig. 7**, there is almost no difference in the specific activity between wild type and mutants of mPTPσ-D1. The specific activities of these mutants vary from 10% to 20% compared with that of the wild type. The most changed mutant is R1416C, of which the specific activity decreases by 50%. Therefore, most of the single amino acid change cannot induce significant activity differences and only the mutant R1416C may bring some activity differences.

Specific activity and kinetic parameters of mPTPσ-D1, mPTPσ-D1D2, hPTPσ-D1, and hPTPσ-D1D2 toward pNPP as the substrate

mPTPσ-D1 mutants have no significant activity differences when compared with the wild type, while the specific activity of mPTPσ-D1 is ~19 folds higher than hPTPσ-D1 specific activity. In order to further confirm the specific activity difference between mPTPσ-D1 and hPTPσ-D1, another widely used PTP substrate pNPP was used to measure the specific activities and kinetic parameters of mPTPσ-D1 and hPTPσ-D1. Interestingly, specific activity, K_m, and k_{cat} of mPTPσ-D1 are almost the same with those of hPTPσ-D1 (**Fig. 8** and **Table 4**), with <30% variation.

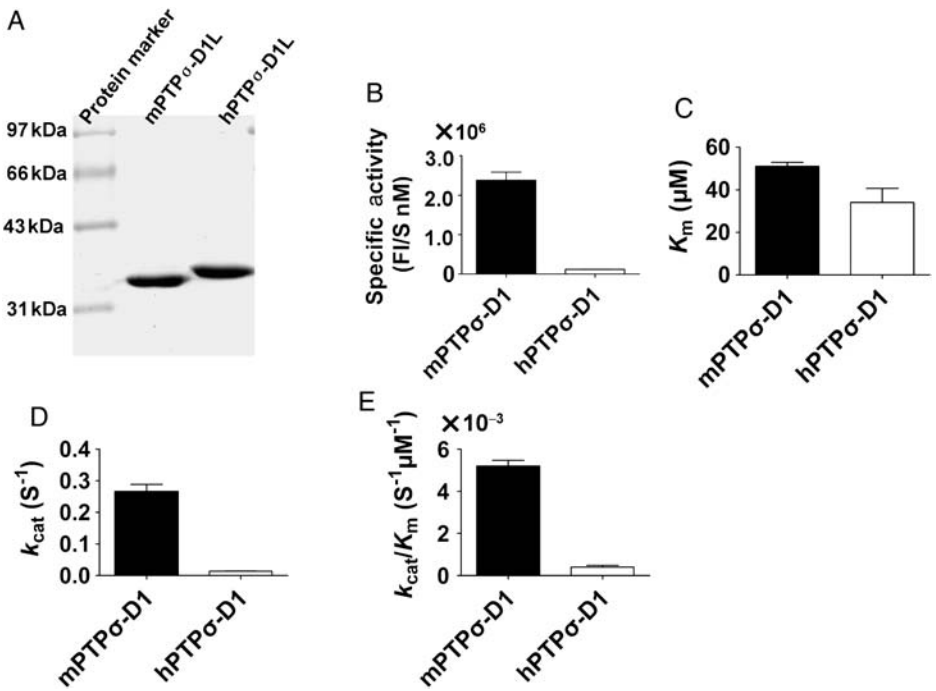

Figure 6 Specific activity and kinetic parameters differences between mPTPσ-D1 and hPTPσ-D1 toward OMFP as the substrate (A) Purification of mPTPσ-D1 and hPTPσ-D1. Lane 1 shows low-molecular-weight protein marker; Lanes 2 and 3 are mPTPσ-D1 and hPTPσ-D1, respectively. Samples were analyzed on a 10% SDS−PAGE and stained with Coomassie Blue G250. The molecular weight of mPTPσ-D1 and hPTPσ-D1 is ∼37 kDa. Purity of them is crystallization grade. (B) Specific activity comparison between mPTPσ-D1 and hPTPσ-D1. The specific activity of mPTPσ-D1 is ∼19 folds higher than that of hPTPσ-D1. (C) K_m comparison between mPTPσ-D1 and hPTPσ-D1. K_m of mPTPσ-D1 is similar to that of hPTPσ-D1. There is 1.6-fold difference in the ratios of K_m of mPTPσ-D1 to hPTPσ-D1. (D) k_{cat} comparison between mPTPσ-D1 and hPTPσ-D1. k_{cat} of mPTPσ-D1 is 20 folds as much as that of hPTPσ-D1. (E) k_{cat}/K_m comparison between mPTPσ-D1 and hPTPσ-D1. k_{cat}/K_m of mPTPσ-D1 is ∼12 folds higher than that of hPTPσ-D1. All data are shown as the mean value ± SD ($n = 3$).

Table 3 Specific activity and kinetic parameters of PTPσ-D1 determined with OMFP as the substrate

	Specific activity (FI/s nM)	K_m (μM)	k_{cat} (S^{-1})	k_{cat}/K_m ($S^{-1}\,M^{-1}$)
mPTPσ-D1L	$2.4 \times 10^6 \pm 2.1 \times 10^5$	$5.1 \times 10^1 \pm 1.7$	$2.7 \times 10^{-1} \pm 2.2 \times 10^{-2}$	$5.2 \times 10^3 \pm 2.8 \times 10^2$
hPTPσ-D1L	$1.2 \times 10^5 \pm 3.6 \times 10^3$	$3.4 \times 10^1 \pm 6.6$	$1.3 \times 10^{-2} \pm 8.4 \times 10^{-4}$	$4.0 \times 10^2 \pm 8.8 \times 10^1$
mPTPσ-D1L/ hPTPσ-D1L	20.2 ± 1.2	1.6 ± 0.5	20.0 ± 1.8	13.4 ± 3.4

These similarities between mPTPσ-D1 and hPTPσ-D1 demonstrate high conservation of PTPσ in mouse and human, which is in accordance with structural similarities between mPTPσ-D1 and hPTPσ-D1. This result is in accordance with results of structural comparison as well as activity comparison between mPTPσ-D1 wide type and mutants. But it does not agree with results from activity difference when using OMFP as the substrate. The discrepancy indicates that mPTPσ-D1 and hPTPσ-D1 have different substrate specificities.

Since specific activity of mPTPσ-D1 and hPTPσ-D1 is similar toward pNPP as the substrate, it could be speculated that the activity of mPTPσ-D1D2 should be identical with that of hPTPσ-D1D2 toward pNPP as the substrate. To compare the activities of mPTPσ-D1D2 and hPTPσ-D1D2, their activities were also measured toward pNPP as the substrate. Their activities and kinetic parameters were measured using the same activity assay method (details described in Materials and Methods). Consistent with those of D1, mPTPσ-D1D2 has almost the same specific activity and kinetic parameters as hPTPσ-D1D2 does. The specific activity and kinetic parameters variations between mPTPσ-D1D2 and hPTPσ-D1D2 are only 10% (**Fig. 9** and **Table 5**). All these similarities are consistent with structural similarities between the two enzymes. In conclusion, specific activity and kinetic parameters similarities between mPTPσ-D1 and hPTPσ-D1 as well as mPTPσ-D1D2 and hPTPσ-D1D2 toward pNPP as the substrate are consistent with conservations of PTPσ intradomains in mouse and human that could be drawn from sequences alignment of

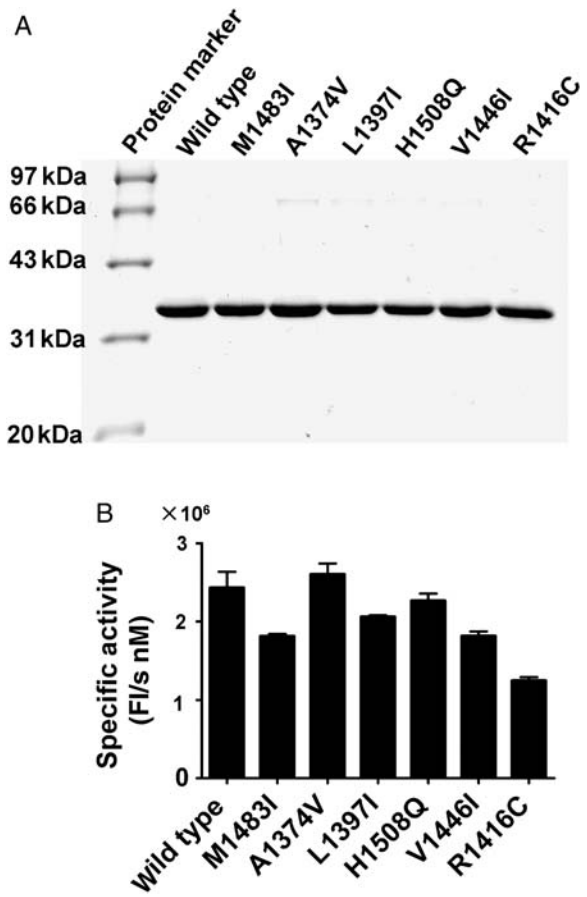

Figure 7 Specific activity comparisons among mPTPσ-D1 wild type and mutants toward OMFP as the substrate (A) Purification of mPTPσ-D1 wild type and mutants. Lane 1 shows low-molecular-weight protein marker; lanes 2–7 are mPTPσ-D1 mutants. Samples were analyzed on a 10% SDS–PAGE, and then the gel was stained with Coomassie blue G250. (B) Specific activities comparison among mPTPσ-D1 wild type and mutants. Specific activities are shown as the mean value ± SD ($n = 3$).

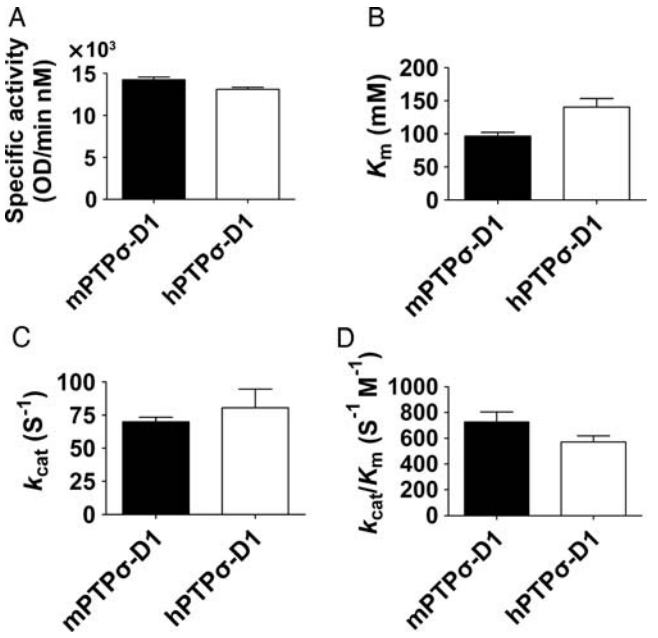

Figure 8 Specific activity and kinetic parameters similarities between mPTPσ-D1 and hPTPσ-D1 toward pNPP as the substrate (A) Specific activity comparison between mPTPσ-D1 and hPTPσ-D1. The specific activity of mPTPσ-D1 is almost comparable with that of hPTPσ-D1. (B) K_m comparison between mPTPσ-D1 and hPTPσ-D1. K_m of mPTPσ-D1 is similar to that of hPTPσ-D1. There is 1.4-fold difference in the ratios of K_m of hPTPσ-D1 to mPTPσ-D1. (C) k_{cat} comparison between mPTPσ-D1 and hPTPσ-D1. k_{cat} of mPTPσ-D1 is 90% as much as that of hPTPσ-D1. (D) k_{cat}/K_m comparison between mPTPσ-D1 and hPTPσ-D1. mPTPσ-D1 has almost the same k_{cat}/K_m as hPTPσ-D1 dose. All data are shown as the mean value ± SD ($n = 3$).

mPTPσ-D1D2 and hPTPσ-D1D2. In addition, different results from pNPP and OMFP suggest that mPTPσ and hPTPσ have different substrate specificities, which indicate that there are tiny differences between mouse PTPσ and human PTPσ.

Discussion

PTPσ plays an important role in the development and regeneration of the nervous system. Here we first reported the well-defined crystal structure of mPTPσ-D1D2 at 2.4 Å resolution. Then we compared the crystal structures of mPTPσ with hPTPσ and found that they have similarities and differences. Furthermore, we also found that mPTPσ-D1D2 has 25-fold higher specific activity when compared with human hPTPσ-D1D2. However, there is no significant activity difference between the mouse and the human enzyme detected with pNPP as the substrate. mPTPσ-D1D2 and hPTPσ-D1D2 as well as mPTPσ-D1 and hPTPσ-D1 have different substrate specificities toward OMFP and pNPP as substrates.

The crystal structure of mPTPσ tandem phosphatase domains we reported here is a monomer in the crystalline state and also behaves as a monomer in solution as judged by analytical gel filtration chromatography (data not shown). This result supports a previous study, in which hPTPσ-D1D2 was reported as a monomer in both crystalline and solution [11]. However, it has been suggested that PTPσ forms homodimers in the cell and that dimerization is required for ligand binding [27]. The apparent discrepancy between these cell-based results and biophysical studies may be explained by demonstrations that dimerization depends, at least in part, on interactions involving the transmembrane segment [27], which is absent from the D1D2 construct used for crystallographic and biophysical studies.

Structural comparison suggests that the crystal structure of mPTPσ-D1D2 is very similar to that of hPTPσ-D1D2, with a RMSD of 0.45 Å for 517 equivalent Cα atoms. However, there are still some differences between the two structures. Of these differences, the first β-sheet (residues 1408–1411 aa) of mPTPσ-D1D2 is shorter than the

Table 4 Specific activity and kinetic parameters of PTPσ-D1 determined with pNPP as the substrate

	Specific activity (OD/min nM)	K_m (mM)	k_{cat} (S^{-1})	k_{cat}/K_m (S^{-1} M^{-1})
mPTPσ-D1	$1.4 \times 10^4 \pm 3.3 \times 10^2$	$9.7 \times 10^1 \pm 5.7$	$7.0 \times 10^1 \pm 3.4$	$7.3 \times 10^2 \pm 7.7 \times 10^1$
hPTPσ-D1	$1.3 \times 10^4 \pm 5.6 \times 10^2$	$1.4 \times 10^2 \pm 1.3 \times 10^1$	$8.0 \times 10^1 \pm 1.4 \times 10^1$	$5.7 \times 10^2 \pm 4.7$
mPTPσ-D1/ hPTPσ-D1	$1.1 \pm 5.0 \times 10^{-3}$	$6.9 \times 10^{-1} \pm 2.4 \times 10^{-2}$	$8.9 \times 10^{-1} \pm 2.0 \times 10^{-1}$	$1.3 \pm 2.4 \times 10^{-1}$

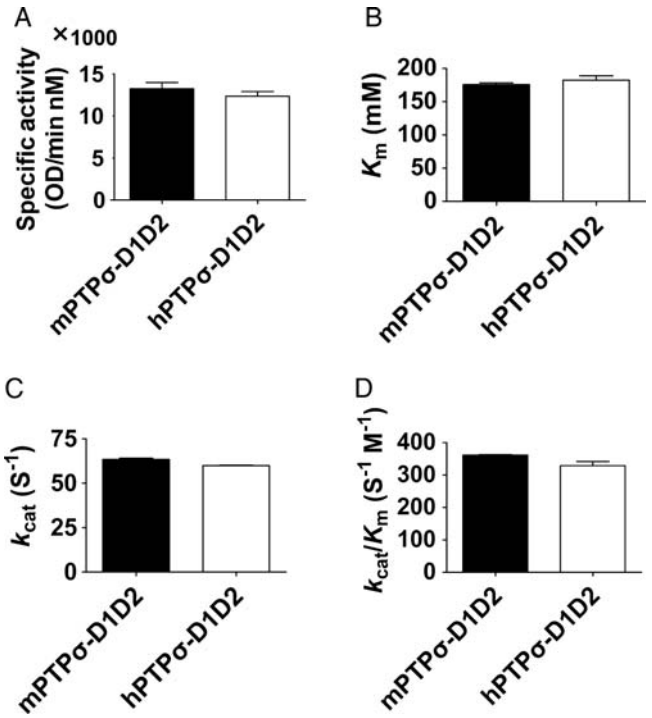

Figure 9 Specific activity and kinetic parameters similarities between mPTPσ-D1D2 and hPTPσ-D1D2 toward pNPP as the substrate (A) Specific activity comparison between mPTPσ-D1D2 and hPTPσ-D1D2. The specific activity of mPTPσ-D1D2 is almost comparable with that of hPTPσ-D1D2. (B) K_m comparison between mPTPσ-D1D2 and hPTPσ-D1D2. K_m of mPTPσ-D1D2 is almost the same as that of hPTPσ-D1D2. (C) k_{cat} comparison between mPTPσ-D1D2 and hPTPσ-D1D2. k_{cat} of mPTPσ-D1D2 is similar to that of hPTPσ-D1D2. (D) k_{cat}/K_m comparison between mPTPσ-D1D2 and hPTPσ-D1D2. k_{cat}/K_m of mPTPσ-D1D2 is very similar to that of hPTPσ-D1D2 with only 10% variation. All data are shown as the mean value ± SD ($n = 3$).

corresponding β-sheet (residues 1446–1454 aa) of hPTPσ-D1D2. Residues 1391–1393 of mPTPσ-D1D2 form a loop but the corresponding residues 1432–1434 in hPTPσ-D1D2 form a β-sheet. Those residues form the back side of the active site and are required for proper folding. Residues 1337–1358 of mPTPσ-D1D2 form two helices but the corresponding residues 1378–1399 in hPTPσ-D1D2 form only one helix, which is beside the active center. These differences make the active center of mPTPσ more flexible than that of hPTPσ and make it easier for mPTPσ to hydrolyze the more complex substrate, such as OMFP. Therefore, these differences are probably one of the reasons for higher specific activity of mPTPσ targeting OMFP as the substrate.

It could be speculated that mPTPσ-D1D2 should have similar activity with hPTPσ-D1D2 from sequences alignment. However, mPTPσ-D1D2 has 25-fold higher activity than hPTPσ-D1D2 does toward OMFP as the substrate. Furthermore, mPTPσ-D1 also has 19-fold higher activity than hPTPσ-D1 does against OMFP. But there are almost no activity differences when detected with pNPP as substrate. It seems to be a discrepancy. Different substrate specificities on OMFP and pNPP may explain this discrepancy. As shown in **Tables 2** and **5**, mPTPσ-D1D2 has ~600-fold higher activity with OMFP than that with pNPP. However, hPTPσ-D1D2 has only ~25-fold higher activity with OMFP than that with pNPP. The 24-fold difference in the ratios of mPTPσ-D1D2 and hPTPσ-D1D2 with these two substrates suggests that mPTPσ-D1D2 and hPTPσ-D1D2 have significant substrate specificities. Comparison of OMFP structure with pNPP structure, it

Table 5 Specific activity and kinetic parameters of PTPσ-D1D2 determined with pNPP as the substrate

	Specific activity (OD/ min nM)	K_m (mM)	k_{cat} (S^{-1})	k_{cat}/K_m (S^{-1} M^{-1})
mPTPσ-D1D2	$1.3 \times 10^4 \pm 7.4 \times 10^2$	$1.8 \times 10^2 \pm 2.7$	$6.3 \times 10^1 \pm 6.9 \times 10^{-1}$	$3.6 \times 10^2 \pm 1.6$
hPTPσ-D1D2	$1.2 \times 10^4 \pm 5.6 \times 10^2$	$1.8 \times 10^2 \pm 6.6$	$6.0 \times 10^1 \pm 2.0 \times 10^{-1}$	$3.3 \times 10^2 \pm 1.3 \times 10^1$
mPTPσ-D1D2/ hPTPσ-D1D2	$1.1 \pm 2.6 \times 10^{-2}$	$1.0 \pm 5.0 \times 10^{-2}$	$1.1 \pm 7.9 \times 10^{-3}$	$1.1 \pm 4.8 \times 10^{-2}$

could be found that the structure of OMFP is more complex. Structural differences between mPTPσ-D1D2 and hPTPσ-D1D2 may result in different position of OMFP between mouse and human PTPσ in the enzyme–substrate complex and hence the different catalytic activity toward OMFP. But it is not for pNPP due to its simple structure. The specific activity and k_{cat} differences between mPTPσ-D1 and hPTPσ-D1 toward OMFP as the substrate are shown the same with those of mPTPσ-D1D2 and hPTPσ-D1D2. The different substrate specificities between mPTPσ-D1D2 and hPTPσ-D1D2 also indicate that PTPσ may have different substrate tendentiousness in physiological state.

Sequences alignment suggests that there are still 20 residues that are different between mPTPσ-D1D2 and hPTPσ-D1D2. Mutagenesis of some of these residues did not identify any other particular single residue that would be responsible for the activity difference except for the mutant R1416C, of which the specific activity decreases by 50%. However, this does not mean these different residues do not affect structures or activities. It is possible that activity differences between mPTPσ-D1D2 and hPTPσ-D1D2 or mPTPσ-D1 and hPTPσ-D1 are not induced by a single amino acid but by the co-action of these residues. Therefore, combined mutants of several amino acids may induce activity differences and further combined mutation is ongoing. For R1416C, of which the specific activity decreases by 50%, it is in a loop in the crystal structure of mouse PTPσ. Therefore, it has some flexibility and mutation from arginine in mouse to cysteine in human may bring about some structural differences, which results in activity differences. But there is a single-nucleotide polymorphism (SNP) in this position in the crystal structure of human PTPσ (PDB code 2FH7), in which the corresponding residue C1419 in human PTPσ used for activity detection is mutated into R1457 in the crystal structure of human PTPσ (PDB code 2FH7) used for structural comparison. As a result, the residue in this position of mPTPσ and hPTPσ used for structural comparison are both arginine and the structural differences between mPTPσ and hPTPσ without SNP in this position caused by this residue difference (R1416 in mouse and C1419 in human) can not be 'observed' in the structural comparison.

In conclusion, we report the well-defined crystal structure of mPTPσ tandem phosphatase domains. Structural comparison suggests that although mPTPσ-D1D2 and hPTPσ-D1D2 are very similar to each other, there are some tiny differences. In addition, mPTPσ-D1D2 has *in vitro* activity differences with hPTPσ-D1D2 against OMFP substrate but their activities are consistent targeting pNPP as the substrate. mPTPσ and hPTPσ have different substrate specificities toward OMFP and pNPP as substrates. Therefore, it could be concluded that mPTPσ has high homology with hPTPσ, but there are still some differences between them.

Acknowledgements

We thank Prof. Jianping Ding at Institute of Biochemistry and Cell Biology (SIBCB), Shanghai Institutes for Biological Sciences (SIBS), Chinese Academy of Sciences (CAS; Shanghai, China) for the guidance of the project. We are grateful to the staff members at the Shanghai Synchrotron Radiation Facility and the Research Center for Structural Biology of SIBCB for technical supports in diffraction data collection and helpful discussion.

Funding

This work was supported by the grants from the Shanghai Science and Technology Community (No. 09DZ2291200), the Chinese Academy of Science 'Strategic Leader in Science and Technology Projects' (No. XDA01040303), and the National Science and Technology Major Project (2007CB914201 and 2009CB940900).

References

1 Fischer EH, Charbonneau H, Cool DE and Tonks NK. Tyrosine phosphatases and their possible interplay with tyrosine kinases. Ciba Found Symp 1992, 164: 132–144.
2 Kotelevets L, van Hengel J, Bruyneel E, Mareel M, van Roy F and Chastre E. The lipid phosphatase activity of PTEN is critical for stabilizing intercellular junctions and reverting invasiveness. J Cell Biol 2001, 155: 1129–1135.
3 Knillova J, Kolar Z and Hlobilkova A. The significance of key regulators of apoptosis in the development and prognosis of prostate carcinoma. II. Products of suppressor genes Rb and PTEN, CDKI, Fas. Biomed Pap Med Fac Univ Palacky Olomouc Czech Repub 2003, 147: 11–17.
4 Den Hertog J and Hunter T. Tight association of GRB2 with receptor protein tyrosine phosphatase alpha is mediated by the SH2 and C terminal SH3 domains. EMBO J 1996, 15: 3016–3027.
5 Asante Appiah E and Kennedy BP. Protein tyrosine phosphatases: the quest for negative regulators of insulin action. Am J Physiol Endocrinol Metab 2003, 284: E663–E670.
6 Zhu Z, Oh SY, Cho YS, Zhang L, Kim YK and Zheng T. Tyrosine phosphatase SHP-1 in allergic and anaphylactic inflammation. Immunol Res 2010, 47: 3–13.
7 Chagnon MJ, Uetani N and Tremblay ML. Functional significance of the LAR receptor protein tyrosine phosphatase family in development and diseases. Biochem Cell Biol 2004, 82: 664–675.
8 Tautz L, Pellecchia M and Mustelin T. Targeting the PTPome in human disease. Expert Opin Ther Targets 2006, 10: 157–177.
9 Alonso A, Sasin J, Bottini N, Friedberg I, Osterman A, Godzik A and Hunter T, *et al*. Protein tyrosine phosphatases in the human genome. Cell 2004, 117: 699–711.
10 Andersen JN, Mortensen OH, Peters GH, Drake PG, Iversen LF, Olsen OH and Jansen PG, *et al*. Structural and evolutionary relationships among protein tyrosine phosphatase domains. Mol Cell Biol 2001, 21: 7117–7136.

11 Almo SC, Bonanno JB, Sauder JM, Emtage S, Dilorenzo TP, Malashkevich V and Wasserman SR, *et al*. Structural genomics of protein phosphatases. J Struct Funct Genomics 2007, 8: 121–140.
12 Johnson KG and Van Vactor D. Receptor protein tyrosine phosphatases in nervous system development. Physiol Rev 2003, 83: 1–24.
13 Aricescu AR, McKinnell IW, Halfter W and Stoker AW. Heparan sulfate proteoglycans are ligands for receptor protein tyrosine phosphatase sigma. Mol Cell Biol 2002, 6: 1881–1892.
14 Fox AN and Zinn K. The heparan sulfate proteoglycan syndecan is an *in vivo* ligand for the *Drosophila* LAR receptor tyrosine phosphatase. Curr Biol 2005, 15: 1701–1711.
15 Johnson KG, Tenney AP, Ghose A, Duckworth AM, Higashi ME, Parfitt K and Marcu O, *et al*. The HSPGs Syndecan and Dallylike bind the receptor phosphatase LAR and exert distinct effects on synaptic development. Neuron 2006, 49: 517–531.
16 Siu R, Fladd C and Rotin D. N-cadherin is an *in vivo* substrate for protein tyrosine phosphatase sigma (PTPsigma) and participates in PTPsigma-mediated inhibition of axon growth. Mol Cell Biol 2007, 27: 208–219.
17 Thompson KM, Uetani N, Manitt C, Elchebly M, Tremblay ML and Kennedy TE. Receptor protein tyrosine phosphatase sigma inhibits axonal regeneration and the rate of axon extension. Mol Cell Neurosci 2003, 23: 681–692.
18 Sapieha PS, Duplan L, Uetani N, Joly S, Tremblay ML, Kennedy TE and Di Polo A. Receptor protein tyrosine phosphatase sigma inhibits axon regrowth in the adult injured CNS. Mol Cell Neurosci 2005, 28: 625–635.
19 Shen Y, Tenney AP, Busch SA, Horn KP, Cuascut FX, Liu K and He Z, *et al*. PTPsigma is a receptor for chondroitin sulfate proteoglycan, an inhibitor of neural regeneration. Science 2009, 326: 592–596.
20 Otwinowski Z and Minor W. Processing of X-ray diffraction data collected in oscillation mode. Method Enzymol 1997, 276: 307–326.
21 Brunger AT, Adams PD, Clore GM, DeLano WL, Gros P, Grosse-Kunstleve RW and Jiang JS, *et al*. Crystallography & NMR system: a new software suite for macromolecular structure determination. Acta Crystallogr D Biol Crystallogr 1998, 54: 905–921.
22 Brunger AT. Version 1.2 of the crystallography and NMR system. Nat Protoc 2007, 2: 2728–2733.
23 Emsley P and Cowtan K. Coot: model-building tools for molecular graphics. Acta Crystallogr D Biol Crystallogr 2004, 60: 2126–2132.
24 Nam HJ, Poy F, Krueger NX, Saito H and Frederick CA. Crystal structure of the tandem phosphatase domains of RPTP LAR. Cell 1999, 97: 449–457.
25 Barr AJ, Ugochukwu E, Lee WH, King ON, Filippakopoulos P, Alfano I and Savitsky P, *et al*. Large-scale structural analysis of the classical human protein tyrosine phosphatome. Cell 2009, 136: 352–363.
26 Nam HJ, Poy F, Saito H and Frederick CA. Structural basis for the function and regulation of the receptor protein tyrosine phosphatase CD45. J Exp Med 2005, 201: 441–452.
27 Lee S, Faux C, Nixon J, Alete D, Chilton J, Hawadle M and Stoker AW. Dimerization of protein tyrosine phosphatase sigma governs both ligand binding and isoform specificity. Mol Cell Biol 2007, 27: 1795–1808.